UC Davis

UC Davis Previously Published Works

Title

Orientation Tuning of Correlated Activity in the Developing Lateral Geniculate Nucleus

Permalink

https://escholarship.org/uc/item/9ch9r15n

Journal

Journal of Neuroscience, 37(48)

ISSN

0270-6474

Authors

Kiley, Caitlin W

Usrey, W Martin

Publication Date

2017-11-29

DOI

10.1523/jneurosci.3762-16.2017

Peer reviewed

eScholarship.org Powered by the California Digital Library
University of California

Systems/Circuits

Orientation Tuning of Correlated Activity in the Developing Lateral Geniculate Nucleus

Caitlin W. Kiley and W. Martin Usrey
Center for Neuroscience, University of California, Davis, California 95618

Neural circuits and the cells that comprise them undergo developmental changes in the spatial organization of their connections and in their temporal response properties. Within the lateral geniculate nucleus (LGN) of the dorsal thalamus, these changes have pronounced effects on the spatiotemporal receptive fields (STRFs) of neurons. An open and unresolved question is how STRF maturation affects stimulus-evoked correlated activity between pairs of LGN neurons during development. This is an important question to answer because stimulus-evoked correlated activity likely plays a role in establishing the specificity of thalamocortical connectivity and the receptive fields (RFs) of postsynaptic cortical neurons. Using multielectrode recording methods and white noise stimuli, we recorded neural activity from ensembles of LGN neurons in cats across early development. As expected, there was a progressive maturation of the spatial and temporal properties of visual responses. Using drifting bar stimuli and cross-correlation analysis, we also determined the orientation-tuning bandwidth of correlated activity between pairs of LGN neurons at different stages of development (Sillito and Jones, 2002; Andolina et al., 2007; Stanley et al., 2012; Kelly et al., 2014). Despite the larger RFs and slower responses of immature LGN neurons compared with mature neurons, our results show that correlated activity in the LGN was as tightly tuned for orientation early in development as it was in the adult. Closer examination revealed this age-invariant orientation tuning of correlated activity likely involves cellular mechanisms related to spike fatigue in young animals and a progressive decrease in response latency with development.

Key words: **cat; development; geniculocortical; LGN; vision**

Significance Statement

Orientation tuning is a fundamental property of neurons in primary visual cortex. An important and unresolved question is how orientation tuning emerges during brain development. This study explores a potential mechanism for the establishment of orientation tuning based on correlated activity patterns among ensembles of maturing neurons in the lateral geniculate nucleus (LGN) of the thalamus. Results show that correlated activity between pairs of LGN neurons is more tightly tuned than predictions based simply on receptive field size, indicating that correlated activity has the properties needed to play an important role in the development of geniculocortical circuits and the emergence of cortical orientation tuning.

Introduction

Correlated activity among neuronal ensembles is known to play a vital role in guiding the specificity and maturation of neuronal circuits. In the visual system, correlated activity can occur independently of visual stimulation, as in the case of retinal waves that emerge before photoreceptor maturation (Meister et al., 1991; Wong et al., 1993; Feller et al., 1997) and in a stimulus-dependent manner, as demonstrated in studies in which eye alignment was altered during the critical period to disrupt interocular correlated activity and typical circuit formation (Hubel and Wiesel, 1965; Hirsch and Spinelli, 1970; Chino et al., 1983; Antonini and Stryker, 1993; White et al., 2001; Hooks and Chen, 2006; Munz et al., 2014). During normal development of the visual system, two factors are predicted to influence the strength and timing of stimulus-dependent correlated activity: the size of neuronal receptive fields (RFs) and the time course of visual responses.

In the lateral geniculate nucleus (LGN) of the dorsal thalamus, neuronal RFs undergo a dramatic reduction in size during development (Daniels et al., 1978; Cai et al., 1997; Tavazoie and Reid, 2000; Tao and Poo, 2005; Koehler et al., 2011), a process largely reflecting a decrease in the number of retinal ganglion cells pro-

Received Dec. 7, 2016; revised Oct. 13, 2017; accepted Oct. 17, 2017.

Author contributions: C.W.K. and W.M.U. designed research; C.W.K. performed research; C.W.K. and W.M.U. analyzed data; C.W.K. and W.M.U. wrote the paper.

This work was supported by the National Institutes of Health (Grants EY013588 and EY016182). We thank Katie Neverkovec, Daniel Sperka, Jeffrey Johnson, Rhonda Oates, and Henry Alitto for expert technical assistance.

The authors declare no competing financial interests.

Correspondence should be addressed to W. Martin Usrey, Center for Neuroscience, University of California, 1544 Newton Court, Davis, CA 95618. E-mail: wmusrey@ucdavis.edu.

DOI:10.1523/JNEUROSCI.3762-16.2017

Copyright © 2017 the authors 0270-6474/17/3711549-10$15.00/0

viding convergent input onto target geniculate neurons (Chen and Regehr, 2000; Jaubert-Miazza et al., 2005). The visual responses of geniculate neurons also become faster and more robust with development due in part to the myelination of retinal axons (Elgeti et al., 1976; Moore et al., 1976) and changes in the biophysical membrane properties of maturing neurons (Monyer et al., 1994; Dunah et al., 1996; Wenzel et al., 1996; Ramoa and Prusky, 1997; Kirson et al., 1999; Misra et al., 2000; Liu and Chen, 2008). Here, we explore the relative maturation of the spatial and temporal properties of visual responses in the developing feline LGN and test the hypothesis that spatiotemporal RF (STRF) refinement dictates the bandwidth of orientation-tuned correlated activity among pairs of geniculate cells. Understanding the mechanisms that underlie the emergence of orientation-tuned ensemble activity is important because this activity is likely to contribute to the developmental refinement of geniculocortical connections (i.e., neurons that fire together, wire together) and the establishment of cortical orientation selectivity.

The larger RFs of LGN neurons in young animals underlies the prediction that oriented stimuli should coexcite pairs of neurons over a broader range of orientations than would occur for more mature neuronal pairs with smaller RFs (Fig. 1). To test this prediction, we collected STRF data from ensembles of LGN neurons at specified ages from 10 d postnatally to adult. With these data, we compared the relative maturation of RF size and response timing. We then used drifting bar stimuli to test the hypothesis that there is a progressive decrease (i.e., sharpening) in the orientation-tuning bandwidth of correlated activity between pairs of neurons across development.

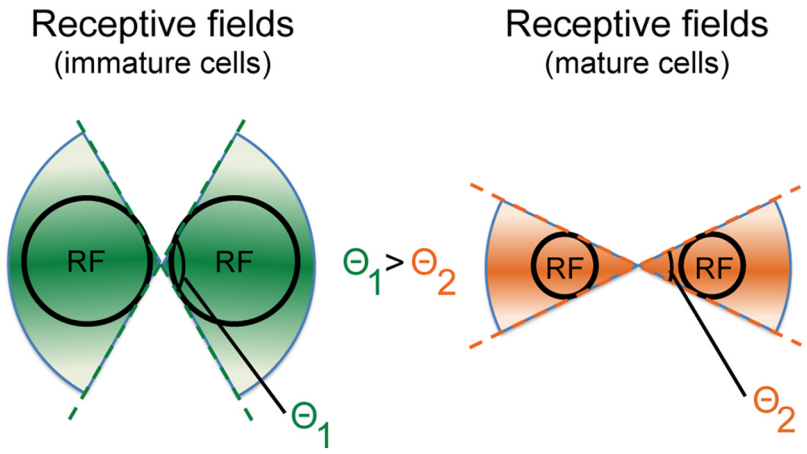

Figure 1. Schematic diagram showing the range of orientations in which a bar stimulus is predicted to coexcite a pair of LGN cells with immature (green) and mature (orange) RFs. In both examples, the circles represent the spatial extent of the RF centers of two LGN cells (same sign). The distance between the centers of the RF centers is the same for both examples. The immature pair of cells with larger RF centers are coexcited by a broader range of angles (θ_1) than the range of angles (θ_2) that coexcite the mature pair of cells with smaller RFs.

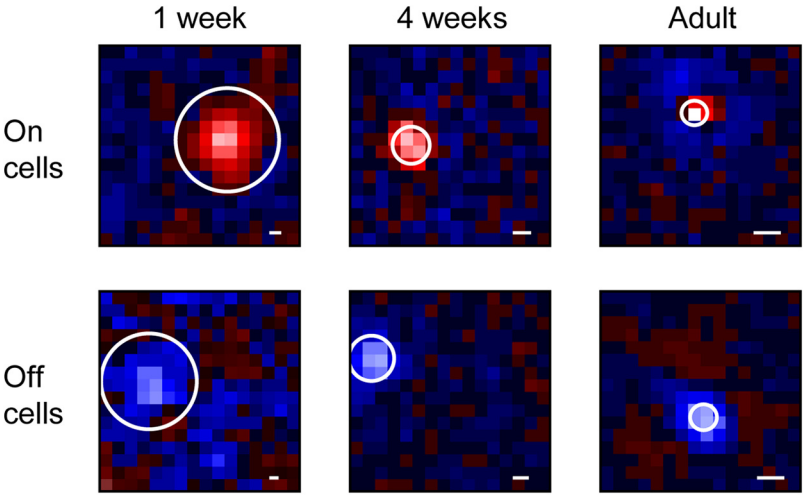

Figure 2. LGN RF center diameter decreases during development. RF maps of on- and off-center cells from 1-week-old, 4-week-old, and adult LGN neurons. RFs were mapped using a white noise stimulus and reverse correlation analysis. On responses are shown in red and off responses are shown in blue; pixel brightness indicates strength of response. White circles demonstrate Gaussian fits to RF center (diameter: 4σ). Scale bars, 1 visual degree.

Contrary to our hypothesis, our results demonstrate that orientation tuning of correlated activity in the LGN is as tightly tuned, if not more so, in young animals as it is in the adult. This result is despite our findings that neuronal RFs in the developing LGN are much larger in size than in the adult and that responses are slower and more sluggish in immature LGN cells. Further investigation revealed this age-invariant orientation tuning of correlated activity likely reflects cellular mechanisms related to spike fatigue in young animals in tandem with a progressive decrease in visual response latency during development. Together, these findings provide key insight into the tight orientation tuning of correlated activity between pairs of geniculate cells in young cats and reveal a substrate with the properties needed for Hebbian mechanisms to guide the development of geniculocortical circuits and the tight orientation tuning reported for simple cells early in cortical development (Moore and Freeman, 2012).

Materials and Methods

Surgery and preparation

All surgical and experimental procedures used in this study were approved by the Institutional Animal Care and Use Committee at the University of California–Davis and were in accordance with U.S. Department of Agriculture and National Institutes of Health guidelines. The study used 22 cats (10 female, 11 male, 1 not documented) aged 10 d to adult. Anesthesia was induced with either isoflurane (0.7–2.0%) in oxygen and nitrous oxide (2:1) or a mixture of ketamine and xylazine (10–22 mg/kg and 1 mg/kg, respectively, i.m.) supplemented with ketamine as needed. A tracheotomy was performed, and anesthesia was maintained with isoflurane (0.7–2.0%) in oxygen and nitrous oxide (2:1). Most animals were placed in a stereotaxic apparatus; the smallest animals were stabilized with a chin rest and head post. Animals were artificially ventilated and monitored for temperature, heart rate, electroencephalogram (EEG), and expired CO_2 throughout the experiment. Physiological measurements indicative of a decrease in anesthesia such as a change in heart rate, expired CO_2, or EEG pattern resulted in an increase in the concentration of isoflurane delivered.

Pupils were dilated using 1% atropine sulfate and nictitating membranes were retracted with 10% phenylephrine. Flurbiprofen sodium

(0.03%) was administered to ensure pupillary dilation. After a midline scalp incision and a small craniotomy made above the LGN, the dura was removed and the craniotomy was filled with agarose. To minimize eye movements, the lateral margin of each eye was exposed and the sclera was glued to a ring mounted on the stereotaxic frame. All wound margins were infused with lidocaine. Eyes were fitted with contact lenses and refracted. At the conclusion of the experiment, the animal was given a lethal dose of Euthasol (100 mg/kg; Virbac Animal Health).

Electrophysiological recordings and visual stimuli

The LGN was located using stereotaxic coordinates from Rose and Goodfellow (1973). Recordings were made from LGN neurons using either single parylene-coated tungsten electrodes (AM Systems) or a seven-channel multielectrode array with platinum-in-quartz electrodes (Thomas Recording). Neuronal responses were amplified, filtered, and recorded to a computer equipped with a Power 1401 data acquisition interface and the Spike 2 software package (Cambridge Electronic Design). Spike isolation was based upon waveform analysis (parameters were established independently for each cell) and the presence of a refractory period as indicated in the autocorrelogram (Usrey et al., 2000, 2003).

Visual stimuli were created with a VSG2/5 or a ViSaGe visual stimulus generator (Cambridge Research Systems) and displayed on a gamma-calibrated CRT monitor with a mean luminance of 38 cd/m^2 and a refresh rate of 120 or 100 Hz.

White noise stimulus. RFs were mapped using a binary white noise stimulus consisting of a 16 × 16 grid of black and white squares. Each square was modulated in time according to an *m*-sequence of length 2^{15}-1 (Reid et al., 1997).

Drifting bar stimulus. A bar stimulus was used to examine correlated firing patterns between cell pairs. Single bars, the length of which extended the length of the monitor and the width of which was set to ~60% of the recorded neuron's RF center size, drifted across a mean gray background at angles ranging between 0 and 170°. We chose to use a bar width of 60% of the RF size to ensure that there were epochs when the stimulus would be restricted within the RFs of recorded cells and to maintain a consistent relationship between bar width and RF sizes. The bars were presented randomly at 10° intervals and drifted across the screen between 12 and 16°/s depending on the temporal response properties of the cells. Each orientation was presented 30 times for a total of 540 trials (18 angles × 30 trials).

Data analysis

Reverse correlation and STRF analysis. STRF maps were generated by applying reverse correlation analysis (Citron et al., 1981; Jones and Palmer, 1987; Sutter, 1992; Reid et al., 1997) on the neuronal responses to the binary white noise stimulus (described above). For each temporal delay between stimulus and response, we calculated the average stimulus that preceded a spike. The resulting STRF can be thought of as the average firing rate of the neuron above or below the mean for each pixel in the stimulus (the impulse response). RF center sizes were quantified as the degrees in visual space corresponding to four times the σ (space constant) of a Gaussian equation fit to the RF at the latency corresponding to the peak response. Impulse responses were calculated by interpolating responses to pixels overlapping the RF center using a piecewise cubic Hermite interpolating polynomial (MATLAB function "pchip"; The MathWorks) in which the center is defined as all contiguous spatial positions having the same sign as the strongest response and 1.5 SDs above the baseline noise value. From the impulse response, response latency was quantified as the time that elapsed between stimulus onset and the peak response. Indices used to compare RF center size and latency at different developmental ages were calculated by dividing the difference of two values by their sums (i.e., RF center size$_{\text{cell A}}$ − RF center size$_{\text{adult average}}$)/(RF center size$_{\text{cell A}}$ + RF center size$_{\text{adult average}}$). All multicomparison analyses were Bonferroni corrected and excluded statistical outliers.

Cross-correlation analysis. To assess the relationship between stimulus orientation and the magnitude of correlated activity between neighboring geniculate neurons of the same sign (i.e., two on-center cells), we generated cross-correlograms from responses to a drifting bar stimulus.

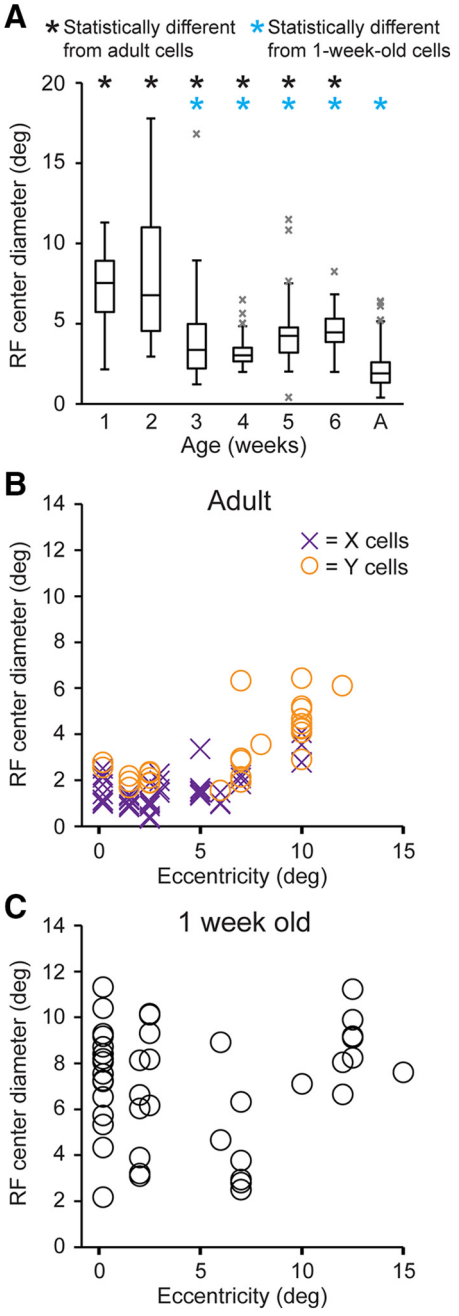

Figure 3. LGN RF center diameter decreases over time and does not correlate with eccentricity during development. ***A***, Box-and-whisker plot of LGN RF center diameter during development. The middle line across the box marks the median, the top and bottom edges the first and third quartile of the population, and the whiskers indicate the minimum and maximum values. Gray X's indicate statistical outliers. Black asterisks identify ages with RF center diameters significantly different from adult animals; blue asterisks identify ages with RF center diameters significantly different from 1-week-old animals ($p = 1.55 \times 10^{-41}$, Kruskal–Wallis, 1 week to adult: $n = 45, 58, 57, 52, 58, 59$, and 68). ***B***, Eccentricity and RF center diameter of X cells ($R^2 = 0.29$, $n = 44$) and Y cells ($R^2 = 0.55$, $n = 29$) in the adult. X cells are marked with an X, Y cells with open circles. X and Y cells were classified based on relative RF size within each neuronal ensemble (Usrey et al., 1999). ***C***, Eccentricity and RF center diameter of neurons at 1 week postnatally ($R^2 = 8.8 \times 10^{-3}$, linear regression, $n = 45$).

Cross-correlograms were generated from responses to each of the 18 angles presented during the drifting bar stimulus and spikes were binned at 0.5 ms. Past work has shown that the spikes of an LGN neuron are more likely to evoke a postsynaptic cortical response when they arrive within 7 ms of a spike from another LGN neuron (Usrey et al., 2000;

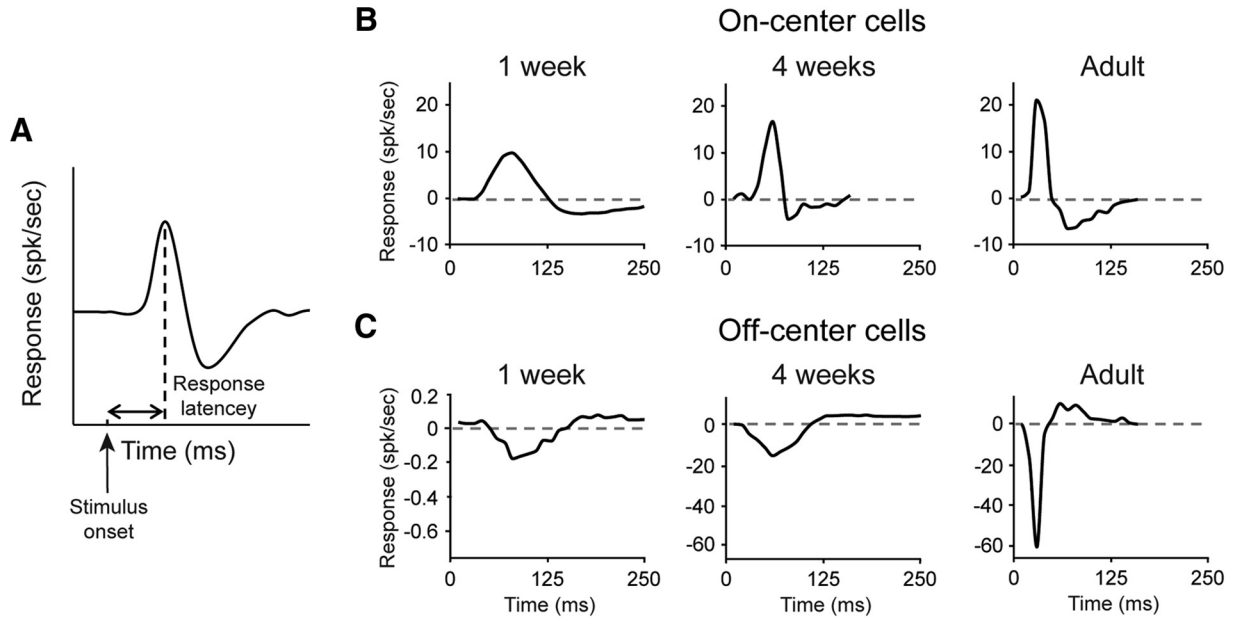

Figure 4. Impulse responses change shape during development. ***A***, Schematic of an LGN cell impulse response. Response latency is the time between stimulus onset and peak response. ***B*** and ***C***, Impulse responses of the cells with RF maps shown in Figure 2. Dotted line marks zero on the *y*-axis.

Usrey, 2002; see also Stanley et al., 2012; Kelly et al., 2014). We therefore integrated spike counts across a ±6.25 ms window of each cross-correlogram to create an orientation-tuning curve for a pair of geniculate neurons using the spikes most likely to drive the cortex. The tuning curves were fit with a Gaussian equation and the half-width at half-height (HWHH) values were extracted and used as a measure of tuning bandwidth.

RF pairs analysis. The distance between the RFs of a cell pair was measured from the strongest pixel of each RF at the peak of each neuron's response. Geniculate cell pairs with RFs farther than 5° apart were not included in the analyses given they are highly unlikely to provide convergent input onto the same cortical cell (Jin et al., 2011). Peak angle of the cell pair tuning curve was defined as the stimulus angle that elicited the maximum response. The spatial angle between RFs was measured with the line used for calculating distance between the RFs.

Response duration and effective RF. Response duration for each cell was defined as the full-width at half-height (FWHH) of the peak of the peristimulus time histogram (PSTH) generated from responses to the drifting bar stimulus. The PSTH peak was fit with an interpolating polynomial using piecewise cubic Hermite interpolating polynomial (MATLAB function "pchip"; The MathWorks) from which we calculated the FWHH of the peak. Cells with PSTH peaks that could not be fit with a polynomial were excluded from the analysis. The effective size of the RF center to the drifting bar stimulus was calculated by multiplying the velocity of the drifting bar to the neuron's response duration. In addition, we calculated where within a neuron's RF the drifting bar was located at the time of the cell's first stimulus-evoked response by multiplying the velocity of the bar stimulus by the cell's response latency.

Results

Spatiotemporal receptive field development

We recorded the spiking activity of 397 LGN neurons in 22 cats at ages 10 d postnatally to adult to determine how the maturation of RFs in both space and time affects the orientation tuning of correlated activity among ensembles of LGN neurons. STRF maps were generated by applying reverse correlation analysis on the responses of neurons to a dense white noise stimulus (see Materials and Methods). Figure 2 shows representative RFs of LGN neurons at three stages of development (1 week, 4 weeks, and adult). In this figure, red pixels indicate regions within the RF excited by bright stimuli (on responses) and blue pixels indicate regions excited by dark stimuli (off responses). RF centers were fitted with a Gaussian equation to quantify RF center size (diameter $= 4\sigma$; represented as circles overlaid on the RF maps). For both the on-center and off-center cells, RF size decreases with age.

Across our sample of cells, RF center size in cats 1–6 weeks postnatally is significantly larger than in adult cats (Fig. 3*A*; $p = 1.55 \times 10^{-41}$, Kruskal–Wallis; 1 week to adult: $n = 45, 58, 57, 52, 58, 59,$ and 68). This finding indicates RF center size does not reach full maturity in cat LGN cells until after 6 weeks postnatally, a finding consistent with previous reports (Daniels et al., 1978; Cai et al., 1997; Tavazoie and Reid, 2000). Importantly, RF center sizes at both 1 and 2 weeks postnatally are statistically different from the other time points, indicating landmark changes in RF refinement between 2 and 3 weeks ($p = 3.2 \times 10^{-11}$, Wilcoxon rank-sum).

To address possible concerns that the differences in RF center size reported here might reflect a sampling bias in eccentricity rather than biological age, we examined RF center size with respect to eccentricity. As shown in Figure 3*B* and consistent with previous reports (Hoffmann et al., 1972; Wilson and Sherman, 1976; Daniels et al., 1978; Tavazoie and Reid, 2000), there is indeed a positive correlation between RF size and distance from area centralis in adult cats (Fig. 3*B*; X cells, $R^2 = 0.29$, $n = 45$; Y cells, $R^2 = 0.55$, $n = 29$). However, this relationship is not present in young animals (Fig. 3*C*; $R^2 = 8.8 \times 10^{-3}$, linear regression, 45 cells). Taken further, these results suggest the mechanisms serving to sculpt RF size during development have the greatest impact on cells with RFs near area centralis.

The STRFs of LGN cells not only show changes in the spatial domain with development, but also in the temporal domain. Again using white noise stimuli and reverse correlation analysis, we determined each cell's temporal response profile (impulse response). Using the impulse response, we then calculated the latency to peak response for each cell (Fig. 4*A*). Impulse response functions for the cells shown in Figure 2 are shown in Figure 4, *B* and *C*. From these examples, it is apparent that there is a decrease in response latency with age. Similar to the decrease in RF size shown in

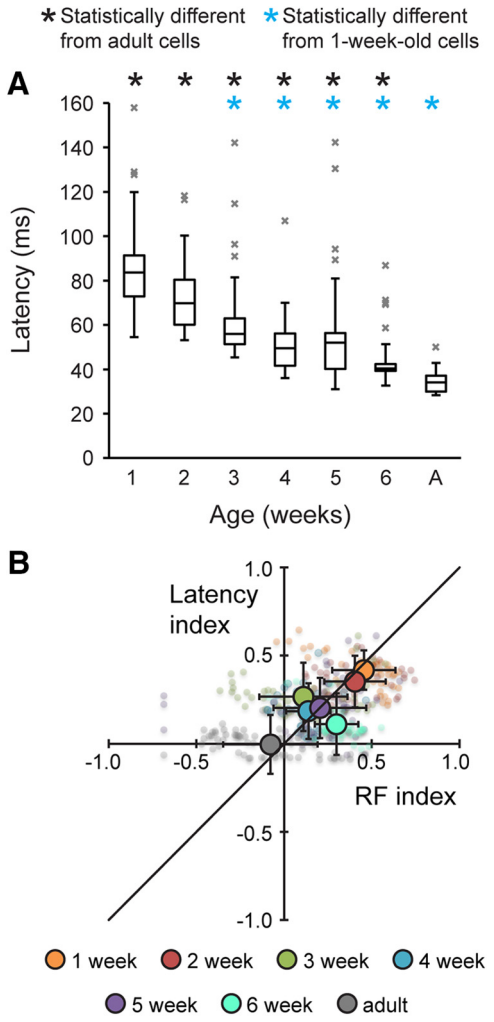

Figure 5. LGN neuron response latency decreases during development. ***A***, Box-and-whisker plot of LGN response latency during development ($p = 6.25 \times 10^{-53}$, Kruskal–Wallis, 1 week to adult: $n = 42, 38, 50, 42, 49, 54$, and 71). Gray X's indicate statistical outliers. Black asterisks identify ages significantly different from adult population, blue asterisks identify ages significantly different from the 1-week-old population. ***B***, Scatter plot of RF center diameter index and latency index. Large circles with SE bars indicate averages for each age group. Zero marks the average value of the adult cell population.

Figure 3*A*, Figure 5*A* shows a decrease in latency throughout the first 6 weeks of postnatal development and also between 6 weeks to adulthood ($p = 6.25 \times 10^{-53}$, Kruskal–Wallis, sample sizes over the range 1 week to adult: $n = 42, 38, 50, 42, 49, 54$, and 71).

To gain greater insight into the relative maturity of LGN RF center size and latency to peak response, we applied an index to compare these cell properties across ages (see Materials and Methods). With this index, values closer to 1.0 signify more immature cell properties and index values closer to zero indicate more adult-like qualities. Figure 5*B* shows the relationship between the relative maturity of RF center size and peak latency. As expected, this figure shows the general trend of index values approaching zero with age.

Correlated firing is more tightly tuned in immature than mature LGN cells

Past work examining geniculocortical communication in adult cats has shown that spikes produced by two LGN neurons are more likely to evoke a postsynaptic cortical response when they occur within 7 ms of each other (Usrey et al., 2000; Usrey, 2002; see also Stanley et al., 2012; Kelly et al., 2014). Because this form of reinforcement could be used by Hebbian mechanisms to establish and/or secure connectivity patterns between LGN and cortex, we wished to know how the orientation tuning of stimulus-evoked correlated activity between pairs of LGN neurons changes with development. To investigate this question, we analyzed the correlated activity of pairs of neurons in the developing and mature LGN to drifting bar stimuli (Sillito and Jones, 2002; Andolina et al., 2007, 2013; see Materials and Methods).

The process of generating orientation-tuning curves of correlated activity is shown in Figure 6, *A–C*, for a representative pair of LGN neurons in the adult cat. In this example, the neurons have RFs that match in sign and are in vertical register (Fig. 6*A*). Given their RF locations, it is expected that a vertical bar drifting over their RFs would be effective at coexciting the two cells. The cross-correlograms in Figure 6*B* illustrate the relationship between the cells' activity patterns when they were stimulated with a variety of stimulus orientations. In these correlograms, the bin at time 0 indicates the occurrence of synchronous spikes between the two cells and bins at positive and negative times indicate the occurrence of spikes with a specific time interval between them. As expected, vertical and near vertical drifting bars evoked more spikes centered at time 0 than horizontal and near horizontal bars. For each pair of cells in this study, we made 18 cross-correlograms from bar stimuli that varied by 10°. Using the total spike count within ± 6.25 ms of 0 in each cross-correlogram (indicated with dashed green lines in Fig. 6*B*), we constructed an orientation-tuning curve of correlated activity for the cell pair. The orientation-tuning curve of correlated activity shown in Figure 6*C* corresponds to the pair of cells illustrated in Figure 6, *A* and *B*; the tuning curves shown in Figure 6, *D–G*, correspond to representative cell pairs from recordings at ages 1–6 weeks. For all tuning curves, we fitted the orientation-tuning curve with a Gaussian equation to determine the orientation-tuning bandwidth of correlated activity (HWHH) (Sillito and Jones, 2002; Andolina et al., 2007, 2013).

We hypothesized that larger RF centers, and therefore younger cells, would yield broader tuning curves because a greater number of orientations would elicit coexcitation from these cell pairs (Fig. 1). In addition, we expected the distance between two RFs to affect the tuning bandwidth such that RFs closer together would also yield broader orientation tuning. The results shown in Figure 7*A* support just one of these predictions. Contrary to our first prediction, orientation-tuning bandwidth during early development is not greater than that in the adult and, if anything, is less than that in the adult at the earliest ages examined ($p < 0.006$, Bonferroni-corrected significance cutoff = 0.008, Kruskal–Wallis). In addition, the distance between RFs does affect tuning bandwidth (second prediction) because measures of HWHH typically decrease as distance increases (Fig. 7*A*). The average HWHH for orientation-tuning curves based on correlated activity between adult LGN cell pairs is quite similar to the HWHH determined from the orientation-tuning curves generated from the spiking activity of adult cortical simple cells (~18–35°) (Sherk and Stryker, 1976; Heggelund and Albus, 1978; Freeman and Ohzawa, 1992; Moore and Freeman, 2012; Sadagopan and Ferster, 2012), as marked by the shaded region in Figure 7*A*.

To address possible concerns that the narrow tuning of correlated activity in immature cell pairs is simply a result of fewer overall spikes produced by the younger cells, we reran our analyses with one-third of the trials (therefore approximately one-third of the spikes) for cell pairs in our youngest ($n = 15$ cells) and oldest age groups ($n = 18$ cells). For this analysis, cell pairs in the young and adult groups were selected such that a comparably

broad range of spike counts (young cells: range = 60–2853 spikes; adult cells: range = 102–2467 spikes) and distances between RF centers (young pairs: 0–1°, 6 pairs; 2–3°, 4 pairs; 3–4°, 5 pairs; adult pairs: 0–1°, 4 pairs; 2–3°, 9 pairs; 3–4°, 5 pairs) were represented. Figure 7*B* demonstrates that this large reduction in spike count does not alter the findings for either group significantly ($p = 0.4553$ for young, $p = 0.6464$ for adult, Wilcoxon rank-sum), thus allaying concern that spike count may have biased the results.

We next examined how well each cell pair's predicted preferred orientation (based on RF locations) matched the pair's preferred orientation (based on joint activity). As shown in Figure 8, the distance between the cells' RFs had a predicable influence on this relationship because cell pairs with RFs closer together show a greater difference in the two orientations than those farther apart. For cell pairs with RF locations >1° apart, predicted preferred orientations based on RF locations are generally within 20° of preferred orientations based on joint activity.

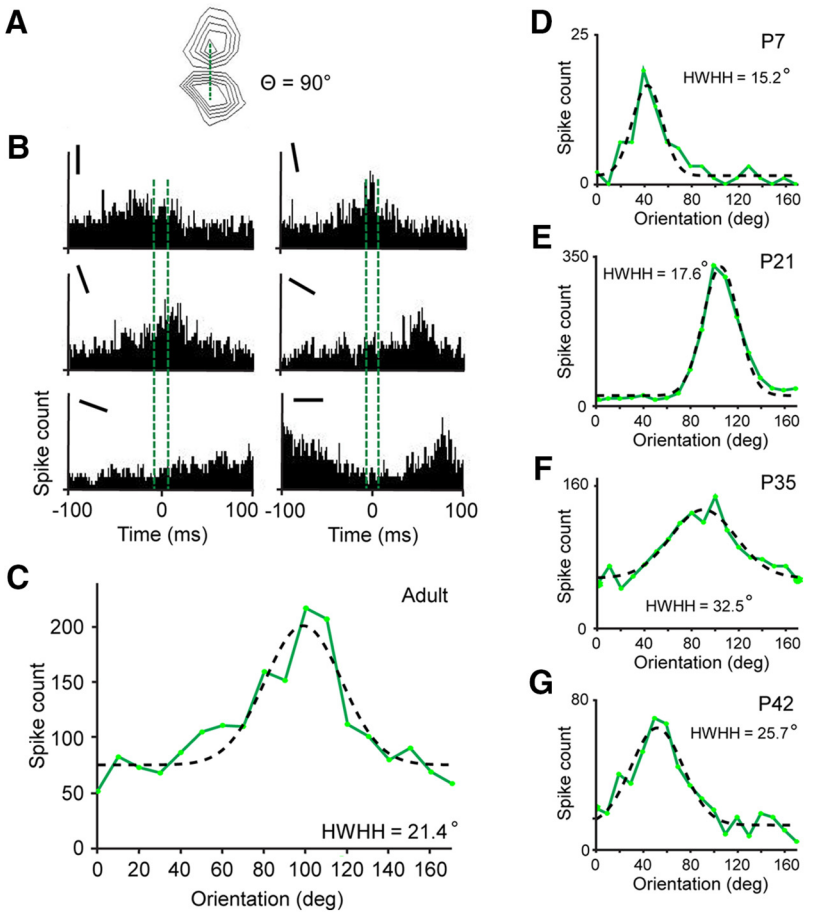

Figure 6. Representative orientation-tuning curves of correlated activity. ***A***, Contour map of two adult LGN RFs. Dotted green line shows the alignment angle of the two RFs. ***B***, Cross-correlograms calculated from the responses of the pair of geniculate neurons with RFs are shown in ***A***. Responses were elicited by a drifting bar stimulus. Angle of the stimulus is depicted in the upper left corner of each cross-correlogram. Dotted lines denote time window of spike integration used to calculate correlated activity tuning curves. ***C***, Orientation-tuning curve resulting from cross-correlograms in ***B***. Green line shows raw data, dotted black line illustrates Gaussian fit. ***D***–***G***, Representative tuning curves for pairs of LGN neurons at ages 1 week, 3 weeks, 5 weeks, and 6 weeks.

Effective RF size leads to tighter tuning of LGN output

To determine what mechanism(s) might underlie the unexpected finding that orientation tuning of LGN correlated activity is not greater in early development than in mature animals, we examined each cell's PSTH during the drifting bar stimulus to gain insight into temporal features of each cell's responses (see Materials and Methods). As shown in Figure 9*A*, there was no difference in PSTH response duration across ages ($p > 0.03$, Bonferroni-corrected significance cutoff = 0.007, Kruskal–Wallis; sample sizes over the range of 1 week to adult: $n = 14$, 26, 42, 32, 30, 46, and 58).

We then used the response duration assessed from drifting bar stimuli to recalculate each neuron's "effective" RF center size, meaning that we redefined the RF center size based on the region of visual space within which the drifting bar elicited a response. Figure 9*B* shows the comparison of "effective" RF sizes determined from the drifting stimulus with RF sizes determined from the white noise stimulus. At all developmental time points before adult, this comparison shows that "effective" RF centers based on drifting-bar stimuli are smaller, on average, than RF centers based on white noise maps ($p < 1.13 \times 10^{-6}$, Wilcoxon rank-sum, 1–6 weeks: $n = 14$, 26, 43, 34, 30, and 46). Interestingly, there is no difference between the two measures in adult LGN cells ($p = 0.0967$, Wilcoxon rank-sum, $n = 60$). These results suggest that spike fatigue to the drifting stimulus in young cells may underlie the smaller RFs (see Discussion). Using the new "effective" RF values, we reevaluated the relationship between RF center size and age. Results of this analysis revealed that RF centers of young cells are not significantly different from those of adult cells ($p > 0.01$, Bonferroni-corrected significance cutoff = 0.007, Kruskal–Wallis).

As a final analysis, we determined where the drifting bar was located within a neuron's RF when that neuron began to fire. Using the edge of the RF center subunit as the zero mark, we calculated the distance between the RF edge and the location of the leading edge of the bar at the moment the neuron started firing. We then converted this distance to the percentage across the RF to allow us to compare values at different ages. Importantly, this analysis revealed that, regardless of age (and thus RF size), neurons began firing when the drifting bar was ~30% across their RF centers (Fig. 9*C*). This finding is consistent with results showing a progressive decrease in response latency with development.

Together, results from this study suggest that response latency and response fatigue work together as LGN RFs mature to ensure that downstream postsynaptic target neurons receive age-invariant, orientation-tuned, correlated activity from pairs of LGN cells.

Discussion

The goal of this study was to determine the relationship between STRF maturation and the development of orientation-tuned correlated activity among ensembles of LGN neurons. Surprisingly, we discovered that immature pairs of LGN neurons are able to provide the cortex with tight orientation-tuned correlated activity despite having large RFs and sluggish responses.

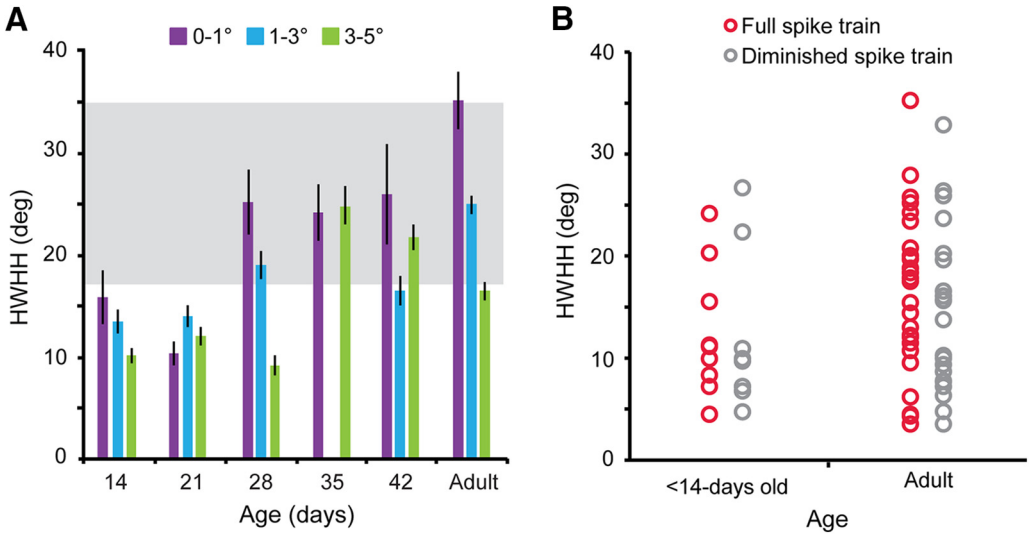

Figure 7. Orientation-tuning bandwidth of correlated activity is tighter in immature LGN cells. ***A***, Plot of average HWHH values from cross-correlogram orientation-tuning curves from cells with RF centers separated by 0–1°, 1–3°, and 3–5°. Shaded gray region demarcates the range for orientation tuning bandwidths reported for simple cells in adult cat visual cortex (Sherk and Stryker, 1976; Heggelund and Albus, 1978; Freeman and Ohzawa, 1992; Moore and Freeman, 2012; Sadagopan and Ferster, 2012). Error bars indicate SE. Data were omitted from categories with <4 cell pairs (i.e., 1–3° in 5-week-old animals). ***B***, HWHH values from LGN neurons in animals <14 d old ($p = 0.4553$, Wilcoxon rank-sum, $n = 14$) and in adult animals ($p = 0.6464$, Wilcoxon rank-sum, $n = 18$). Open red circles represent complete dataset, open gray circles represent dataset with 33% of total spikes.

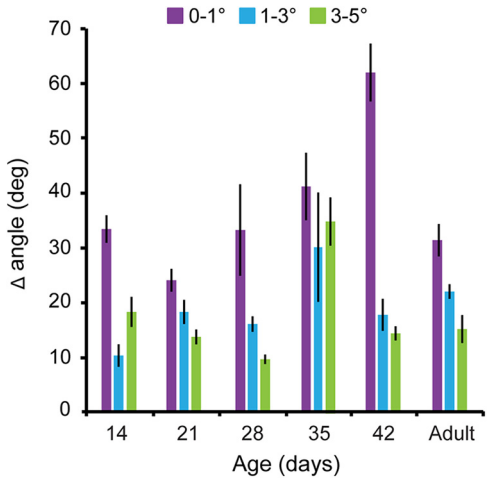

Figure 8. Preferred angle for orientation tuning of correlated activity reflects the spatial relationship of RF pairs. Shown is a bar plot of the average absolute difference between predicted and measured preferred angles for cell pairs with RF centers separated by 0–1°, 1–3°, and 3–5°.

Consistent with past results, our data demonstrate that LGN RFs in young animals are larger than those in the adult (Daniels et al., 1978; Cai et al., 1997; Tavazoie and Reid, 2000; Tao and Poo, 2005; Koehler et al., 2011). This finding is likely not due to poor optics because the RFs of retinal ganglion cells in age-matched young animals are similar in size to those in adults (Tavazoie and Reid, 2000). Instead, RF size appears to depend on the number of retinal ganglion cells providing convergent input to individual LGN neurons. In support of this view, *in vitro* physiological investigations of retinogeniculate synapse maturation describe an early exuberance of convergent connections that is followed by a developmental pruning and reduction in the number of retinal ganglion cells that provide convergent input to individual LGN neurons (Chen and Regehr, 2000; Jaubert-Miazza et al., 2005). Separately, anatomical studies show axonal terminal endings resembling growth cones in cats 2 weeks postnatally, suggesting that both axon remodeling and target finding are still occurring at this age. By 3 weeks of age, when our data showed a large decrease in RF size, axon terminal swellings begin to form adult-like crenulations indicative of stabilized connections (Mason, 1982). This trend of maturing terminal endings continues for weeks, as does RF sculpting, both in the LGN and the visual cortex (DeAngelis et al., 1993).

Along with the developmental refinement of LGN RFs that occurs in the spatial domain, the visual responses of LGN neurons also undergo a progressive maturation in the temporal domain. Using reverse correlation analysis and white noise stimuli, our results show response latency decreases dramatically between 2 and 3 weeks postnatally during the period when myelination of retinal axons reaches the LGN (Elgeti et al., 1976; Moore et al., 1976). After this time, response latency continues to decrease, but more gradually, coinciding in time with when the optic nerve reaches 80% myelination (Cragg, 1975; Moore et al., 1976).

Results from this study also demonstrate that the orientation-tuning bandwidth of correlated activity is similar for LGN cell pairs in young and mature animals. This finding was unanticipated, especially in light of the larger RF centers mapped with noise stimuli in younger neurons. However, further analysis revealed that age-invariant orientation tuning of correlated activity can be accounted for by interactions between the transient nature of visual responses in young neurons to drifting bar stimuli and the longer response latencies of young neurons. Through mechanisms that likely include adaptation and/or spike fatigue (Hubel and Wiesel, 1963; Huttenlocher, 1970; Buisseret and Imbert, 1976; Daniels et al., 1978; Beckmann and Albus, 1982), young neurons respond more transiently to drifting stimuli than mature neurons. Therefore, young neurons respond to a drifting stimulus only when it passes through a subsection of the RF, thereby decreasing the effective size of the RF. This effect, coupled with a delay in the visual response, centers the reduced, "effective" RF to the center of the RF map determined with white noise stimuli. A similar phenomenon has been reported for macaque area MT

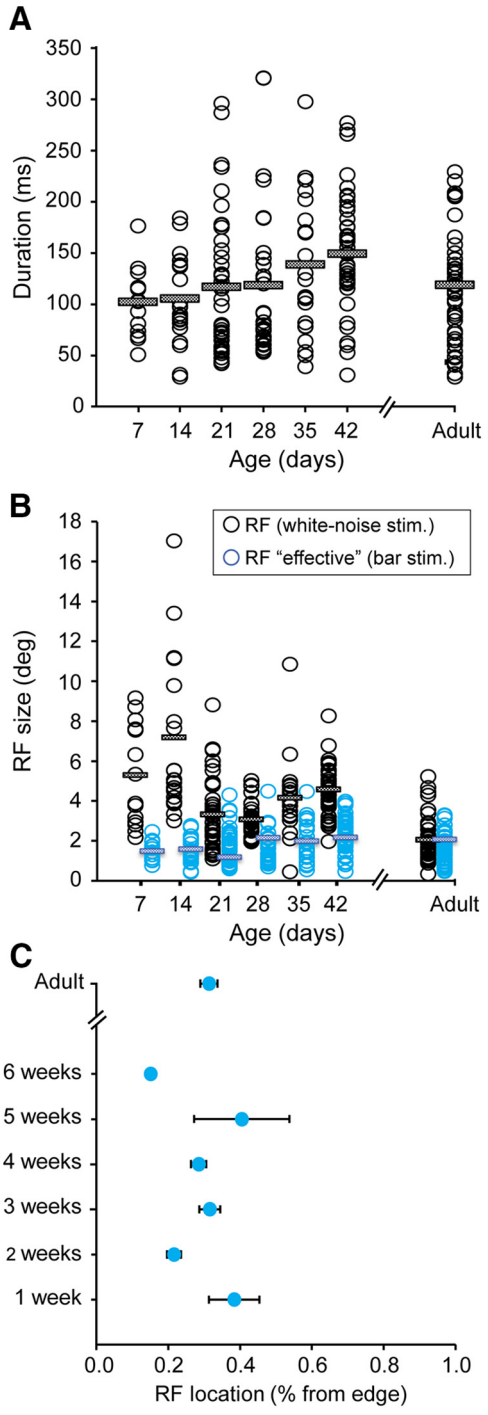

Figure 9. Response duration alters "effective" RF center size of developing LGN neurons. ***A***, Scatter plot of response duration elicited by drifting bar stimulus. Response duration was measured as the FWHH of the PSTH peak. Values were averaged across all stimulus trials. Horizontal bars show duration average for each age group (1 week to adult: $n = 14, 26, 42, 32, 30, 46,$ and 58). ***B***, Scatter plot of RF center diameter and "effective" RF center diameter during development. At all developmental stages, the white-noise mapped RF center size is larger than the effective RF center ($p < 1.13 \times 10^{-6}$, Wilcoxon rank-sum, 1–6 weeks: $n = 14, 26, 43, 34, 30,$ and 46). There is no difference in adult RF center size values using the two methods ($p = 0.0967$, Wilcoxon rank-sum, $n = 60$). Across all seven developmental time points, there is not a difference in effective RF size. Open black circles represent RF center diameter calculated from a Gaussian fit, open blue circles represent the effective RF center size based on response duration to a drifting bar stimulus (see Materials and Methods). ***C***, Plot of average stimulus location with respect to the edge of the RF center at the time the neuron begins to fire. Error bars indicate SE.

during high-noise visual processing, although this finding addressed space only (Kumano and Uka, 2012).

Interestingly, the tuning bandwidth of correlated LGN activity that we report for the youngest animals is significantly less than that reported for individual cortical simple cells of similarly aged cats (Bonds, 1979; Albus and Wolf, 1984; 1985; Freeman and Ohzawa, 1992; Moore and Freeman, 2012; Braastad and Heggelund, 1985). There are several likely reasons for the difference. First, simple cells are known to receive input from more than two LGN cells (Tanaka, 1983; Peters and Payne, 1993; Reid and Alonso, 1995; Usrey et al., 2000) and, although we know little about the spatial extent of LGN inputs to individual simple cells in kitten cortex, it is likely that there is a relationship between the size of the ensemble and the broader tuning bandwidth of young simple cells. Second, synaptic delays between the LGN and cortex normalize around 4 weeks postnatally and myelination of the optic radiations occurs between 3 and 6 weeks (Beckmann and Albus, 1982). Changes in these temporal properties may affect tuning bandwidth in the cortex in ways that our data do not capture.

We suggest that the response fatigue that we and others observed in young LGN neurons (Hubel and Wiesel, 1963; Huttenlocher, 1970; Buisseret and Imbert, 1976; Daniels et al., 1978; Beckmann and Albus, 1982) may play an important role in circuit development. Given that LGN neurons are not fully mature at 6 weeks, downstream cortical cells would have to wait weeks after eye opening before spatially restricted, tightly correlated activity could be transmitted from the LGN. Along these lines, we know that manipulations such as lid suturing, which severely degrades image quality and acts similarly to a low-pass filter, perturb the development of orientation selectivity and direction selectivity in cortex (Pettigrew, 1974; Sherk and Stryker, 1976; Chapman and Stryker, 1993; White et al., 2001). To ensure that the pace of visual development is not delayed by large RFs, the system appears to compensate by limiting the duration of stimulus-evoked responses in young neurons. In this way, the RFs of young neurons are operationally smaller and can produce precise correlated activity nearly indistinguishable from that of adult neurons. This strategy would serve to accelerate the maturation of orientation selectivity, which is known to develop early, between 1 and 4 weeks postnatally in the cat (Buisseret and Imbert, 1976; Albus and Wolf, 1984; Braastad and Heggelund, 1985; Freeman and Ohzawa, 1992; Moore and Freeman, 2012).

Stability of orientation tuning appears to be important for both the developing and adult brain. In the adult, the orientation-tuning bandwidth of cortical neurons is invariant to both stimulus contrast and temporal frequency (Sclar and Freeman, 1982; Skottun et al., 1987; Anderson et al., 2000; Alitto and Usrey, 2004; Moore et al., 2005; Finn et al., 2007; Preibe and Ferster, 2008). Here, we show that the orientation-tuning bandwidth of LGN ensemble activity is also invariant to age. We suggest that this tight orientation tuning of ensemble activity observed in early postnatal development plays a role in the early establishment of orientation tuning in cortex. Given that LGN spikes are more likely to evoke a postsynaptic spike in the cortex when they arrive shortly after (<7 ms) a spike from another LGN neuron (Usrey et al., 2000; Usrey and Alitto, 2015; Stanley et al., 2012; Kelly et al., 2014), we suggest that the mature-like orientation tuning of LGN ensemble activity seen in early development serves as a substrate for Hebbian mechanisms to use in the establishment of the highly precise patterns of geniculocortical connections observed in the adult (Reid and Alonso, 1995; Alonso et al., 2001).

References

Albus K, Wolf W (1984) Early post-natal development of neuronal function in the kitten's visual cortex: a laminar analysis. J Physiol 348:153–185. CrossRef Medline

Alitto HJ, Usrey WM (2004) Influence of contrast on orientation and temporal frequency tuning in ferret primary visual cortex. J Neurophysiol 91:2797–2808. CrossRef Medline

Alonso J-M, Usrey WM, Reid RC (2001) Rules of connectivity between geniculate cells and simple cells in cat primary visual cortex. J Neurosc 21:4002–4015. Medline

Anderson JS, Lampl I, Gillespie DC, Ferster D (2000) The contribution of noise to contrast invariance of orientation tuning in cat visual cortex. Science 290:1968–1972. CrossRef Medline

Andolina IM, Jones HE, Wang W, Sillito AM (2007) Corticothalamic feedback enhances stimulus response precision in the visual system. Proc Natl Acad Sci U S A 104:1685–1690. CrossRef Medline

Andolina IM, Jones HE, Sillito AM (2013) Effects of cortical feedback on the spatial properties of relay cells in the lateral geniculate nucleus. J Neurophysiol 109:889–899. Medline

Antonini A, Stryker MP (1993) Rapid remodeling of axonal arbors in the visual cortex. Science 260:1819–1821. CrossRef Medline

Beckmann R, Albus K (1982) The geniculocortical system in the early postnatal kitten: An electrophysiological investigation. Exp Brain Res 47:49–56. Medline

Bonds AB (1979) Development of orientation tuning in the visual cortex of kittens. In: Developmental neurobiology of vision (Freeman RD, ed), pp 31–41. Boston, MA: Springer.

Braastad BO, Heggelund P (1985) Development of spatial receptive-field organization and orientation selectivity in kitten striate cortex. J Neurophysiol 53:1158–1178. Medline

Buisseret P, Imbert M (1976) Visual cortical cells: Their developmental properties in normal and dark reared kittens. J Physiol 255:511–525. CrossRef Medline

Cai D, DeAngelis GC, Freeman RD (1997) Spatiotemporal receptive field organization in the lateral geniculate nucleus of cats and kittens. J Neurophysiol 78:1045–1061. Medline

Chapman B, Stryker MP (1993) Development of orientation selectivity in ferret visual cortex and effects of deprivation. J Neurosci 13:5251–5262. Medline

Chen C, Regehr WG (2000) Developmental remodeling of the retinogeniculate synapse. Neuron 28:955–966. CrossRef Medline

Chino YM, Shansky MS, Jankowski WL, Banser FA (1983) Effects of rearing kittens with convergent strabismus on development of receptive-field properties in striate cortex neurons. J Neurophysiol 50:265–286. Medline

Citron MC, Kroeker JP, McCann GD (1981) Nonlinear interactions in ganglion cell receptive fields. J Neurophysiol 46:1161–1176. Medline

Cragg BG (1975) The development of synapses in the visual system of the cat. J Comp Neurol 160:147–166. CrossRef Medline

Daniels JD, Pettigrew JD, Norman JL (1978) Development of single-neuron responses in kitten's lateral geniculate nucleus. J Neurophysiol 41:1373–1393. Medline

DeAngelis GC, Ohzawa I, Freeman RD (1993) Spatiotemporal organization of simple-cell receptive fields in the cat's striate cortex I. General characteristics and postnatal development. J Neurophysiol 69:1091–1117. Medline

Dunah AW, Yasuda RP, Wang YH, Luo J, Dávila-García M, Gbadegesin M, Vicini S, Wolfe BB (1996) Regional and ontogenic expression of the NMDA receptor subunit NR2D protein in rat brain using a subunit-specific antibody. J Neurochem 67:2335–2345. Medline

Elgeti H, Elgeti R, Fleischhauer K (1976) Postnatal growth of the dorsal lateral geniculate nucleus of the cat. Anat Embryol 149:1–13. CrossRef Medline

Feller MB, Butts DA, Aaron HL, Rokhsar DS, Shatz CJ (1997) Dynamic processes shape spatiotemporal properties of retinal waves. Neuron 19:293–306. CrossRef Medline

Finn IM, Priebe NJ, Ferster D (2007) The emergence of contrast-invariant orientation tuning in simple cells of cat visual cortex. Neuron 54:137–152. CrossRef Medline

Freeman RD, Ohzawa I (1992) Development of binocular vision in the kitten's striate cortex. J Neurosci 12:4721–4736. Medline

Heggelund P, Albus K (1978) Response variability and orientation discrimination of single cells in striate cortex of cat. Exp Brain Res 32:197–211. Medline

Hirsch HV, Spinelli DN (1970) Visual experience modifies distribution of horizontally and vertically oriented receptive fields in cats. Science 168:869–871. CrossRef Medline

Hoffmann KP, Stone J, Sherman SM (1972) Relay of receptive-field properties in dorsal lateral geniculate nucleus of the cat. J Neurophysiol 35:518–531. Medline

Hooks BM, Chen C (2006) Distinct roles for spontaneous and visual activity in remodeling of the retinogeniculate synapse. Neuron 52:281–291. CrossRef Medline

Hubel DH, Wiesel TN (1963) Receptive fields of cells in striate cortex of very young, visually inexperienced kittens. J Neurophyiol 26:994–1002. Medline

Hubel DH, Wiesel TN (1965) Binocular interaction in striate cortex of kittens reared with artificial squint. J Neurophysiol 28:1041–1059. Medline

Huttenlocher PR (1970) Myelination and the development of function in immature pyramidal tract. Exp Neurol 29:405–415. CrossRef Medline

Jaubert-Miazza L, Green E, Lo FS, Bui K, Mills J, Guido W (2005) Structural and functional composition of developing retinogeniculate pathway in the mouse. Vis Neurosci 22:661–676. CrossRef Medline

Jin J, Wang Y, Swadlow HA, Alonso JM (2011) Population receptive fields of ON and OFF thalamic inputs to an orientation column in visual cortex. Nat Neurosci 14:232–238. CrossRef Medline

Jones JP, Palmer LA (1987) The two-dimensional spatial structure of simple receptive fields in cat striate cortex. J Neurophysiol 58:1187–1211. Medline

Kelly ST, Kremkow J, Jin J, Wang Y, Wang Q, Alonso JM, Stanley GB (2014) The role of thalamic population synchrony in the emergence of cortical feature selectivity. PLoS Comput Biol 10:e1003418. CrossRef Medline

Kirson ED, Schirra C, Konnerth A, Yaari Y (1999) Early postnatal switch in magnesium sensitivity of NMDA receptors in rat CA1 pyramidal cells. J Physiol 521:99–111. Medline

Koehler CL, Akimov NP, Rentería RC (2011) Receptive field center size decreases and firing properties mature in ON and OFF retinal ganglion cells after eye opening in the mouse. J Neurophysiol 106:895–904. CrossRef Medline

Kumano H, Uka T (2012) Reduction in receptive field size of macaque MT neurons in the presence of visual noise. J Neurophysiol 108:215–226. CrossRef Medline

Liu X, Chen C (2008) Different roles for AMPA and NMDA receptors in transmission at the immature retinogeniculate synapse. J Neurophysiol 99:629–643. CrossRef Medline

Mason CA (1982) Development of terminal arbors of retinogeniculate axons in the kitten–I. Light microscopical observations. Neuroscience 7:541–559. CrossRef Medline

Meister M, Wong RO, Baylor DA, Shatz CJ (1991) Synchronous bursts of action potentials in ganglion cells of the developing mammalian retina. Science 252:939–943. CrossRef Medline

Misra C, Brickley SG, Wyllie DJ, Cull-Candy SG (2000) Slow deactivation kinetics of NMDA receptors containing NR1 and NR2D subunits in rat cerebellar Purkinje cells. J Physiol 525:299–305. CrossRef Medline

Monyer H, Burnashev N, Laurie DJ, Sakmann B, Seeburg PH (1994) Developmental and regional expression in the rat brain and functional properties of four NMDA receptors. Neuron 12:529–540. CrossRef Medline

Moore BD 4th, Freeman RD (2012) Development of orientation tuning in simple cells of primary visual cortex. J Neurophysiol 107:2506–2516. CrossRef Medline

Moore BD 4th, Alitto HJ, Usrey WM (2005) Orientation tuning, but not direction selectivity, is invariant to temporal frequency in primary visual cortex. J Neurophysiol 94:1336–1345. CrossRef Medline

Moore CL, Kalil R, Richards W (1976) Development of myelination in optic tract of the cat. J Comp Neurol 165:125–136. CrossRef Medline

Munz M, Gobert D, Schohl A, Poquérusse J, Podgorski K, Spratt P, Ruthazer ES (2014) Rapid Hebbian axonal remodeling mediated by visual stimulation. Science 344:904–909. CrossRef Medline

Peters A, Payne BR (1993) Numerical relationships between geniculocortical afferents and pyramidal cell modules in cat primary visual cortex. Cereb Cortex 3:69–78. CrossRef Medline

Pettigrew JD (1974) The effect of visual experience on the development of stimulus specificity by kitten cortical neurons. J Physiol 237:49–74. CrossRef Medline

Priebe NJ, Ferster D (2008) Inhibition, spike threshold, and stimulus selectivity in primary visual cortex. Neuron 57:482–497. CrossRef Medline

Ramoa AS, Prusky G (1997) Retinal activity regulates developmental switches in functional properties and ifenprodil sensitivity of NMDA receptors in the lateral geniculate nucleus. Brain Res Dev Brain Res 101:165–175. Medline

Reid RC, Alonso JM (1995) Specificity of monosynaptic connections from thalamus to visual cortex. Nature 378:281–284. CrossRef Medline

Reid RC, Victor JD, Shapley RM (1997) The use of m-sequences in the analysis of visual neurons: linear receptive field properties. Vis Neurosci 14:1015–1027. CrossRef Medline

Rose GH, Goodfellow EF (1973) A stereotaxic atlas of the kitten brain: coordinates of 104 selected structures. Los Angeles: University of California Brain Information Service/Brain Research Institute.

Sadagopan S, Ferster D (2012) Feedforward origins of response variability underlying contrast invariant orientation tuning in cat visual cortex. Neuron 74:911–923. CrossRef Medline

Sclar G, Freeman RD (1982) Orientation selectivity in the cat's striate cortex is invariant with stimulus contrast. Exp Brain Res 46:457–461. CrossRef Medline

Sherk H, Stryker MP (1976) Quantitative study of cortical orientation selectivity in visually inexperienced kitten. J Neurophysiol 39:63–70. Medline

Sillito AM, Jones HE (2002) Corticothalamic interactions in the transfer of visual information. Philos Trans R Soc Lond B Biol Sci 357:1739–1752. CrossRef Medline

Skottun BC, Bradley A, Sclar G, Ohzawa I, Freeman RD (1987) The effects of contrast on visual orientation and spatial frequency discrimination: a comparison of single cells and behavior. J Neurophysiol 57:773–786. Medline

Stanley GB, Jin J, Wang Y, Desbordes G, Wang Q, Black MJ, Alonso JM (2012) Visual orientation and directional selectivity through thalamic synchrony. J Neurosci 32:9073–9088. CrossRef Medline

Sutter EE (1992) A deterministic approach to nonlinear systems analysis. In: Nonlinear Vision: Determination of Neural Receptive Fields, Function, and Networks (Pinter R, Nabet B, eds), pp 171–220. Cleveland, OH: CRC Press.

Tanaka K (1983) Cross-correlation analysis of geniculostriate neuronal relationships in cats. J Neurophysiol 49:1303–1318. Medline

Tao HW, Poo MM (2005) Activity-dependent matching of excitatory and inhibitory inputs during refinement of visual receptive fields. Neuron 45:829–836. CrossRef Medline

Tavazoie SF, Reid RC (2000) Diverse receptive fields in the lateral geniculate nucleus during thalamocortical development. Nat Neuroscience 3:608–616. CrossRef Medline

Usrey WM (2002) Spike timing and visual processing in the retinogeniculocortical pathway. Philos Trans R Soc Lond B Biol Sci 357:1729–1737. CrossRef Medline

Usrey WM, Alonso JM, Reid RC (2000) Synaptic interactions between thalamic inputs to simple cells in cat visual cortex. J Neurosci 20:5461–5467. Medline

Usrey WM, Sceniak MP, Chapman B (2003) Receptive fields and response properties of neurons in layer 4 of ferret visual cortex. J Neurophysiol 89:1003–1015. Medline

Usrey WM, Alitto HJ (2015) Visual functions of the thalamus. Ann Rev Vis Sci 1:351–371. CrossRef Medline

Usrey WM, Reppas JB, Reid RC (1999) Specificity and strength of retinogeniculate connections. J Neurophysiol 82:3527–3540. Medline

Wenzel A, Villa M, Mohler H, Benke D (1996) Developmental and regional expression of NMDA receptor subtypes containing the NR2D subunit in rat brain. J Neurochem 66:1240–1248. Medline

White LE, Coppola DM, Fitzpatrick D (2001) The contribution of sensory experience to the maturation of orientation selectivity in ferret visual cortex. Nature 411:1049–1052. CrossRef Medline

Wilson JR, Sherman SM (1976) Receptive-field characteristics of neurons in cat striate cortex: changes with visual field eccentricity. J Neurophysiol 39:512–533. Medline

Wong RO, Meister M, Shatz CJ (1993) Transient period of correlated bursting activity during development of the mammalian retina. Neuron 11:923–938. CrossRef Medline